Effects of PMU Bias Errors In System Inertia Estimation

Demy Alexander, Sachinth Viththarachchige, Praveesh Yoganathan, Arun Manoharan, Visvakumar Aravinthan
Department of Electrical and Computer Engineering
Wichita State University
Wichita, KS, USA
daalexander@shockers.wichita.edu

***Abstract*—Recent advancements in large, distributed, and often unobservable resources at the grid edge have introduced unprecedented challenges for system operators. Industry practices such as lowering operational thresholds and enhancing damping mechanisms underscore the severity of sudden variations that may trigger under-frequency load shedding. A promising approach to improve situational awareness is quasi–real-time inertia estimation, which has become a central focus in recent literature. Among the methods investigated, phasor measurement unit data has emerged as a key tool for estimating online inertia. However, a critical limitation remains largely overlooked: bias errors in frequency estimation. This work addresses this gap by quantifying the impact of phasor bias errors on inertia estimation. Based on the case studies, this work demonstrates that PMU-based phasors can yield significant and inconsistent estimation errors under disturbances, even with a total vector error of only 1%. These findings highlight the need to account for bias errors and to develop new methods that mitigate their influence in inertia estimation.**

***Index Terms*—frequency nadir; inertia estimation; Phasor Measurement Unit; bias error; ROCOF.**

I. Introduction

Increased reliance on renewable energy resources has created challenges for system operators. System operations with stable frequency have become a challenge due to variability in the generation and reduced inertia. The addition of electronically controlled grid edge resources such as data centers has intensified these concerns. One of the examples is the frequent load change in the data centers (AI data centers). Compared to traditional data centers, the computational load can change faster which impacts the cooling system energy consumption [1]. Both fluctuations not only affect the system load but also impact the frequency response.

In a recent NERC report, it was stated that the data center demand can have ramping rates up to $1.9\ \mathrm{p.u./s}$ during the AI training transitions. The lack of inertia from electronically controlled resources reduces the grid's ability to ride through these disturbances, which further highlights the problem [2]. Furthermore, system events can trigger huge system wide oscillations in the presence of electronically controlled loads. This was evident in a recent event within Dominion Energy which saw a 1500 MW swing due to loss of a data center [3]. When weather impacts on the data center load are included, a two-time-scale disturbance can be observed. Faster changes are due to the electronic load control and slower changes due to changes in cooling load.

To reduce the grid impacts of large electronically controlled loads, greater emphasis should be placed on improving situational awareness and implementing dynamic control strategies. Table I summarizes recent operational changes that system operators have adopted to enhance both real time visibility and responsive control.

TABLE I. Recent Changes to Operational Limits

Entity	Parameter	Old Practice	New Practice
NERC [4], [5]	Disturbance ride through	Defined mainly for generators & IBRs	Stricter threshold for large loads (>25MW) with location requirements
ENTSO-E (Europe) [6], [7]	Voltage ride through	1.118 pu – 1.15 pu (20–60 mins response time)	Strict monitoring; emphasis on Voltage Immunity and faster response.
	Frequency ride through	General ride through	Remains same with specific thresholds for data center > 10 MW
AEMO (Australia) [8], [9]	Voltage ride through	Load trips, no specific ride through	Mandatory VRT curves must remain connected during specified events.
	Frequency ride through	Load trips, no specific ride through	Must ride through disturbances down to 47 Hz and up to 52 Hz.
ERCOT [10], [11]	Frequency ride through	Load shed in 3 stages	Load shed in 5 stages
	Voltage ride through	Passive / No Standard	Must ride through ~9 cycles / 0.15s
SPP [12], [13]	Voltage ride through	Passive / No Standard	Specified for different voltage levels
	Frequency ride through	Not specified for large loads	NERC standard PRC-029-1 with stricter case by case

From Table I, it can be observed that as electronically controlled grid edge resources increase greater emphasis is given to situational awareness. One aspect of situational

979-8-3315-8138-1

awareness is having access to on-line system inertia, and localized inertia response.

Recent literature shows significant interest in online inertia estimation. Based on extensive literature these techniques rely on SCADA and/or phaser measurement unit (PMU) data [14]-[16] . Park et. al. and Ghosal et. al have demonstrated that SCADA based inertia estimation is good for synchronous generator inertia estimation, but when electronically controlled loads are incorporated their sampling rate is insufficient [17], [18].

Traditionally, PMU based on-line inertia estimation methods focused on generators. For example, Gorbunov et. al. proposed a method to minimize the mean squared error in inertia estimation and tested on the simulated data [19]. Sanchez-Ocampo et. al. proposed an algorithm based on autoregressive-moving average with exogenous terms for online estimation of system inertia and used IEEE test system to validate their results [20]. Lavanya et. al. proposed an online inertia estimation method with Q-learning and tested in IEEE test system [21]. Even though different approaches are presented in the literature none of them used actual measured PMU data which can be prone to errors.

Recent literature has identified inherent bias errors in PMU measurements that can affect estimation or predictions [22]. None of the studies have examined the impact of inherent bias errors of PMU measurements on on-line inertia estimation. Hence, in this paper, the effect of PMU bias errors on inertia estimation has been studied. The focus of this paper is limited to the PMU bias errors as the other type of errors have been widely investigated in existing literature.

II. Modelling PMU Bias Error

The phasor representation of two phasors is given in Figure 1. The actual k^{th} phasor is denoted as $\mathbf{X}_{\boldsymbol{k}}$ and the k^{th} PMU estimated phasor is given as $\widehat{\mathbf{X}}_{\boldsymbol{k}}$. The estimated phasor may reside anywhere within the circular error region. Figure 1(a) illustrates a scenario where the error regions do not intersect, whereas Figure 1(b) depicts overlapping regions. This intersection is particularly critical; it can effectively reverse the sign of the angle difference, leading to significant inaccuracies in frequency and power output calculations. According to the IEC/IEEE 60255-118-1:2018 standard [23], the Total Vector Error (TVE) can be calculated as (1) where $\mathbf{X}_r$ and $\mathbf{X}_i$ are real and imaginary components of the phasor.

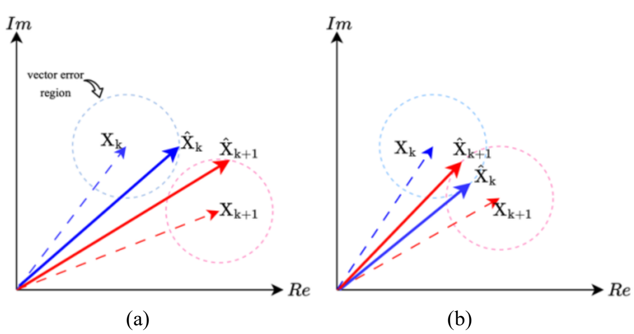

Figure 1. Representation of two consecutive phasors. (a) Non-intersecting error region. (b) Intersecting error region.

$$TVE = \sqrt{\frac{\left(\widehat{\mathbf{X}}_r - \mathbf{X}_r\right)^2 + \left(\widehat{\mathbf{X}}_i - \mathbf{X}_i\right)^2}{\mathbf{X}_r^2 + \mathbf{X}_i^2}} \tag{1}$$

The PMU measurement errors can be classified as the bias error, relative error and the noise caused by other peripheral devices [24]. The errors in the phase angle estimation can happen due to delays in the time synchronization, or due to the input signal having off-nominal frequency. Most prior literature has focused on zero-mean Gaussian noise errors. In contrast, for applications such as online inertia estimation, which rely on the system's dynamic behavior, bias errors arising from off-nominal system frequencies can be prevalent.

A. Phasor Estimation at Off-Nominal System Frequency

Although the *phasor* is a steady state concept, it is unavoidable to rely on phasor approximates originating from PMUs even in cases of quasi-steady states, or during disturbances, to keep track of the system frequency. For a system assumed to be operating at its nominal frequency ω_0 (120π rads^{-1} for a 60 Hz system), discrete Fourier transform (DFT) is set to perform the processing based on cosines and sines of this nominal frequency. At any given time, an input signal $x(t)$ to a PMU could have a frequency ω that is different from ω_0 (i.e., $\omega = \omega_0 + \Delta\omega$).

$x(t)$ can be expressed in phasor form as,

$$x(t) = \sqrt{2}\mathrm{Re}\{\boldsymbol{X}e^{j\omega t}\} \tag{2}$$

Where, $\boldsymbol{X}$ denotes the correct value of the phasor in off-nominal frequency, and Re{·} is the real value. The real value of the phasor can be written as in (3) by taking the average of the complex number and its conjugate ($\boldsymbol{X}^*$).

$$x(t) = \frac{1}{\sqrt{2}}(\boldsymbol{X}e^{j\omega t} + \boldsymbol{X}^* e^{-j\omega t}) \tag{3}$$

The phasor resulted from PMU (X′) due to the off-nominal frequency of the signal can be represented as (4). Where Δt is the sampling window with a sampling frequency f_s and $\boldsymbol{A}, \boldsymbol{B}$ are complex attenuation gains which depend on the deviation of the actual and nominal frequency[25]. The above complex attenuation gains results in the bias error of the PMU measurements. The complex attenuation gains mentioned above result in a bias error within the PMU measurements. Eliminating this error requires knowledge of the actual frequency of the signal. However, since frequency estimations are carried out using phasor angle measurements from the PMU, this error inherently persists in the measurements.

$$\mathrm{X}' = \boldsymbol{A}\boldsymbol{X}e^{j(\omega-\omega_o)\Delta t} + \boldsymbol{B}\boldsymbol{X}^* e^{-jr(\omega+\omega_o)\Delta t} \tag{4}$$

III. Inertia Estimation Under PMU Bias Errors

Historically, inertia of the power system is defined as the energy stored in the rotating machines. The inertia constant of a generator represents the amount of time the generator takes to fully spend the amount of energy stored in it if supplied at its

979-8-3315-8138-1

rated power [26]. Even though the inertia constant of a machine is considered as a fixed value, in reality, it is not a fixed value. Using the swing equation, the inertia of the system can be calculated as in (5). The change in generator output in MW is denoted as ΔP, the rated power of the machine in MW is given as S_{base} and the system rated frequency is denoted as f_0. The rate of change of frequency (ROCOF) is given in Hz/s.

$$H = \frac{-\Delta P}{2 \times ROCOF \times S_{base}} f_0 \tag{5}$$

A typical frequency response of a generator due to a load increment disturbance is shown in Figure 2. The decline in frequency should be arrested before the frequency reaches the under-frequency load shedding (UFLS) limits to avoid any protection relay operations. The inertial response of the generator is faster than the primary frequency response. Combination of primary frequency response and the inertial response help in arresting the frequency drop before it reaches the UFLS limits. For accurate inertia estimation, the ROCOF and the ΔP values before the primary frequency response should be considered.

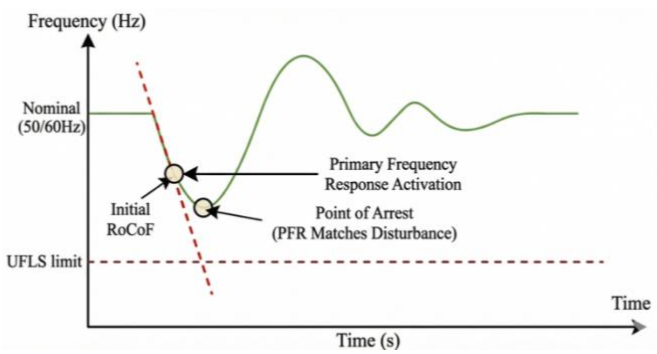

Figure 2. Typical frequency reponse of a generator during a disturbance

The frequency measurement is carried out in PMU by relating the phase angle of the phasor θ with the fundamental frequency f_0. The frequency measurement formulation provided in the standard [23] is given by (6). Here, the estimated phasor angle $\hat{\theta}(t)$ can be decomposed into two parts: the actual phasor angle θ_m, and the bias error counterpart of the angle θ_b. If $\theta_b(t)$ remains constant between estimation windows in the PMU, or $\theta_b(t)$ is negligible compared to $\theta_m(t)$ then $\dot{\theta}_b(t)$ will tend towards zero. However, since the bias errors are not constant over time, $\dot{\theta}_b(t)$ can become a larger value leading to a frequency error. Even a small frequency error can lead to a larger error in the ROCOF calculation since the inertia estimation window is short. Moreover, if the error regions of two consecutive phasors overlap, the difference between phasor angles may vary in the opposite direction. This can cause the frequency estimate to shift incorrectly, resulting in highly inaccurate inertia values.

$$\hat{f}(t) = f_0 + \frac{1}{2\pi} \frac{d[\hat{\theta}(t)]}{dt} \tag{6}$$

$$\hat{\theta}(t) = \theta_m(t) + \theta_b(t) \tag{7}$$

$$\hat{f}(t) = f_0 + \frac{1}{2\pi}\frac{d[\theta_m(t)]}{dt} + \frac{1}{2\pi}\frac{d[\theta_b(t)]}{dt} \tag{8}$$

$$\overline{ROCOF}(t) = \frac{d[\hat{f}(t)]}{dt} = \frac{1}{2\pi}\frac{d^2[\theta_m(t)]}{dt^2} + \frac{1}{2\pi}\frac{d^2[\theta_b(t)]}{dt^2} \tag{9}$$

IV. Numerical Analysis

A. Simulation Scanerios

In this study, modified versions of the IEEE 9 bus system and IEEE 39 bus system are used to perform inertia calculations for different scenarios. The generators are modeled as detailed synchronous generators in PSCAD. Data center demand variations are modeled using both step and ramp load changes as shown in Figure 3. The scenarios considered in this study are provided in Table II. The scenario of step load increase represents the data center behavior of switching GPUs from idle to operation while the ramping behavior represents the data center power usage during the transition from training and saving checkpoint progress[2].

TABLE II. Simulation Scenarios

Scenario	Description
1	Step load increase
2	Ramping load change of 2 pu/s
3	Ramping load change of 0.8 pu/s

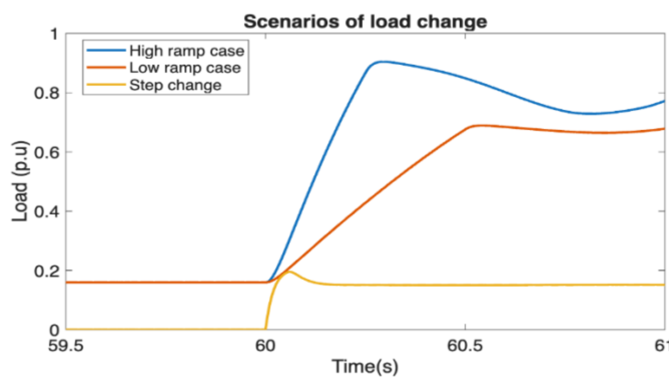

Figure 3. Different data center load variation scenarios

B. Results And Analysis

The frequency response of the system seen at different buses for step load increase is shown in Figure 4. The frequency response of a single generator in IEEE 9 bus system for above mentioned load scenarios is given in Figure 5. Generators 2 and 3 have rated capacities of 200 MVA and 100 MVA, respectively. Generator 3 exhibits a faster frequency response than Generator 2, as the load disturbance is applied to a bus electrically closer to Generator 3.

The phase angles and the voltage magnitudes resulted from the PSCAD simulations represent the actual phasors. To mimic the PMU measurements, an error vector of magnitude 0.01 and an angle varying in the range of $[-\pi, \pi]$ radians is introduced. Based on the simulation results of IEEE 9 bus system, the resulted phasor angle along with the actual phase angle is plotted in Figure 6. The frequency estimated using the actual phase angles and the phase angles derived from error

979-8-3315-8138-1

incorporated phasor measurements is given in Figure 7. It is noticed that the errors in frequency range from 0 to 0.42% for the given scenario. The variation in ROCOF based on actual and estimated frequency measurements are given in Figure 8.

The inertia constant is determined at the generator bus using both actual and phasor-estimated frequency measurements. While the selection of the estimation time window is critical—specifically, it must capture the inertial response preceding the generator's primary frequency response—this study prioritizes the impact of PMU errors. Consequently, the absolute accuracy of the time window selection is not the primary focus. By consistently applying the same time window to both actual and PMU-derived calculations, the analysis isolates the error attributable to PMU measurements, allowing the specific influence of the time window to be neglected. Table III presents the estimated inertia constants for generator buses in the IEEE 9-bus and 39-bus test systems. Across all scenarios, the calculation errors are both significant and inconsistent. These results underscore the adverse impact of potential bias error—even within the allowable PMU TVE range—on the accuracy of online inertia estimation.

TABLE III. INERTIA ESTIMATION RESULTS FOR DIFFERENT SCENARIOS

Scenarios	Inertia Constant Estimation (s)					
	IEEE 9 bus system			*IEEE 39 bus system*		
	Actual	*PMU*	*Error (%)*	*Actual*	*PMU*	*Error (%)*
1	1.85	0.95	-49	0.17	0.18	2
2	1.95	8.08	314	0.09	0.01	-90
3	2.91	2.23	-23	0.21	0.02	-89

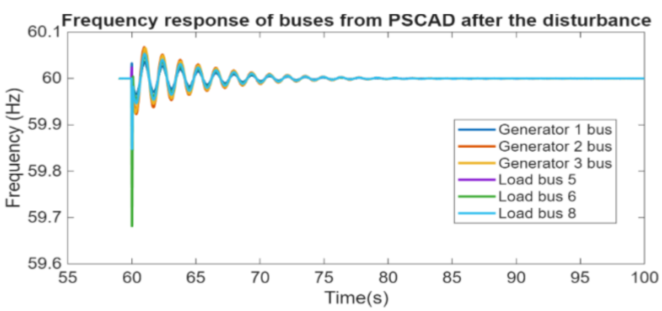

Figure 4. Frequency response at buses after the disturbance

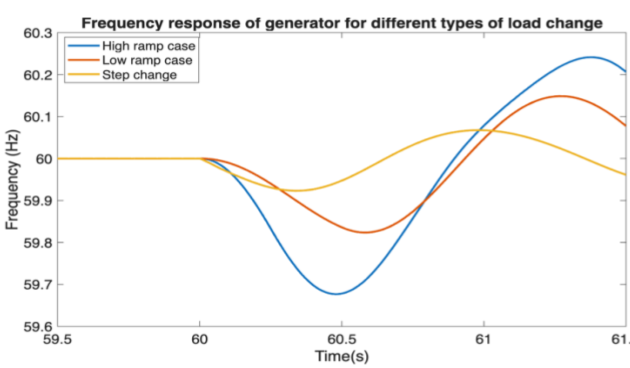

Figure 5. Frequency response at a generator bus for different disturbance types

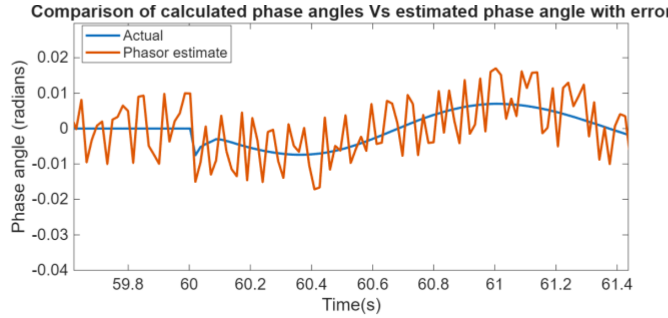

Figure 6. Actual vs. Estimated phase angles

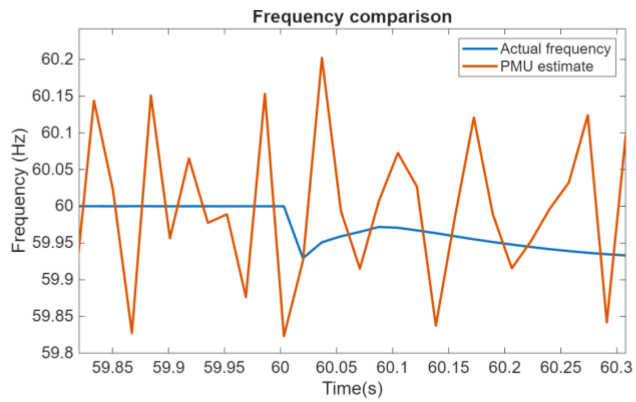

Figure 7. Actual vs. Estimated frequency at a generator bus

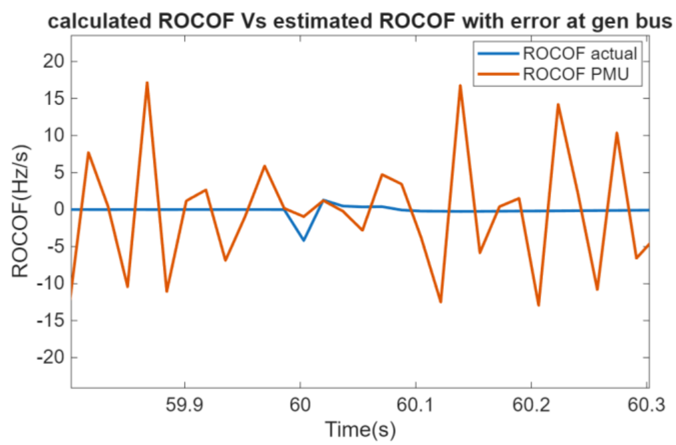

Figure 8. Actual vs. Estimated ROCOF at a generator bus

V. CONCLUSION

The significance of online inertia estimation has grown substantially due to the potential for large load swings in future power systems. While PMUs provide operators with granular data for improved decision-making, a critical and understudied challenge is the bias error caused by off-nominal frequency characteristics. For precision-dependent applications like inertia estimation, these errors can significantly distort results. This study demonstrates that even with a compliant 1% TVE, inertia estimates can deviate by more than 300%. This magnitude of error highlights a gap in the present literature, where PMU bias in inertia estimation is often overlooked. Consequently, future work will focus on characterizing these

979-8-3315-8138-1

errors using vendor-specific PMU measurements and developing mitigation techniques to ensure estimation accuracy

REFERENCES

[1] "DOE Releases New Report Evaluating Increase in Electricity Demand from Data Centers," *Energy.gov*, Dec. 20, 2024. https://www.energy.gov/articles/doe-releases-new-report-evaluating-increase-electricity-demand-data-centers\

[2] NERC, "Characterization and risks of emerging large loads," Jun. 2025. [Online]. Available: https://www.nerc.com/globalassets/who-we-are/standing-committees/rstc/whitepaper-characteristics-and-risks-of-emerging-large-loads.pdf

[3] C. Waldoch, "Byte Blackouts: How large data center loads are surfacing new issues," *Grid Status Exports*, Apr. 18, 2025. https://blog.gridstatus.io/byte-blackouts-large-data-center-loads-new-issues-pjm/

[4] Northeast Power Coordinating Council, "Automatic Underfrequency Load Shedding," Regional Reliability Standard PRC-006-NPCC-2, Apr. 2020. [Online]. Available: https://www.nerc.com/standards/reliability-standards/prc/prc-006-npcc-2

[5] NERC, "Large Load Interconnection, Study, Commissioning, and Operations," NERC Level 2 Industry Recommendation, Sept. 9, 2025.

[6] European Commission, "Commission Regulation (EU) 2016/1388 of 17 August 2016 establishing a Network Code on Demand Connection," *Official Journal of the European Union*, vol. 59, no. L 223, pp. 10–54, Aug. 18, 2016. [Online]. Available: http://data.europa.eu/eli/reg/2016/1388/oj

[7] ENTSO-E, "ENTSO-E Position on the Need for National Connection Requirements to Ensure EU Power System Stability," ENTSO-E, Brussels, Belgium, Position Paper, Dec. 22, 2025. [Online]. Available: https://www.entsoe.eu/2025/12/22/entso-e-position-on-the-need-for-national-connection-requirements-to-ensure-eu-power-system-stability/

[8] Australian Energy Market Commission (AEMC), "Improving the NEM access standards – Package 2," Consultation Paper, Sydney, NSW, Australia, May 8, 2025. [Online]. Available: https://www.aemc.gov.au/rule-changes/improving-nem-access-standards-package-2

[9] Australian Energy Market Commission (AEMC), "National Electricity Rules Version 243," Jan. 1, 2026. [Online]. Available: https://energy-rules.aemc.gov.au/ner/current/chapter-5#Schedule%205.3

[10] Electric Reliability Council of Texas, "Update to EEA Trigger Levels," Nodal Protocol Revision Request (NPRR) 1176, Oct. 2023. [Online]. Available: https://www.ercot.com/mktrules/issues/NPRR1176

[11] Electric Reliability Council of Texas, "Change UFLS Stages and Load Relief Amounts," Nodal Operating Guide Revision Request (NOGRR) 247, Oct. 2023. [Online]. Available: https://www.ercot.com/mktrules/issues/NOGRR247

[12] Southwest Power Pool, "Integrate & Operate High Impact Large Loads," Revision Request (RR) 696, Sep. 2025. [Online]. Available: https://www.spp.org/spp-documents-filings/?id=21069

[13] NERC, "Project 2020-02 Modifications to PRC-024 (Generator Ride-through) and PRC-029-1," NERC Reliability Standards, Sept. 2024. [Online].Available:https://www.nerc.com/globalassets/standards/reliability-standards/prc/2020-02_prc-024-4_prc-029-1_implementation_plan_final.pdf

[14] S. Dulal, M. Olama, N. L. Thotakura, and Y. Liu, "Inertia estimation for power grids: A review of methods, challenges, and future prospects," *Applied Energy*, vol. 407, p. 127333, Mar. 2026, doi: 10.1016/j.apenergy.2025.127333.

[15] A. Mehrzad et al., "Inertia in renewable power systems: a review of estimation methods and practical implementation," *Renewable and Sustainable Energy Reviews*, vol. 226, p. 116246, Jan. 2026, doi: 10.1016/j.rser.2025.116246.

[16] N. S. Ghiasi, R. Hadidi, M. Nouri and B. Chowdhury, "A Comprehensive Review of Online Inertia Estimation Techniques for Modern Power Systems with Renewable Penetration," *2025 IEEE Power & Energy Society General Meeting (PESGM)*, Austin, TX, USA, 2025, pp. 1-5, doi: 10.1109/PESGM52009.2025.11225489.

[17] Park, J.-K., Lee, Y., & Lee, S.-R. (2025). Residual inertia estimation method for KEPCO power systems using PMU and EMS-based frequency response analysis. *Processes*, *13*(7), 2012. https://doi.org/10.3390/pr13072012

[18] Ghosal, M., & Rao, V. (2019). Fusion of multirate measurements for nonlinear dynamic state estimation of the power systems. *IEEE Transactions on Smart Grid*, *10*(1), 216–226. https://doi.org/10.1109/tsg.2017.2737359

[19] A. Gorbunov, A. Dymarsky and J. Bialek, "Estimation of Parameters of a Dynamic Generator Model From Modal PMU Measurements," in *IEEE Transactions on Power Systems*, vol. 35, no. 1, pp. 53-62, Jan. 2020, doi: 10.1109/TPWRS.2019.2925127.

[20] A. Sanchez-Ocampo et al., "Real-time inertia estimation via ARMAX model representation and synchrophasor measurements," in *IEEE Latin America Transactions*, vol. 23, no. 5, pp. 405-414, May 2025, doi: 10.1109/TLA.2025.10974367.

[21] L. Lavanya and K. S. Swarup, "Continuous Real-Time Estimation of Power System Inertia Using Energy Variations and Q-Learning," in *IEEE Open Journal of Instrumentation and Measurement*, vol. 2, pp. 1-11, 2023, Art no. 9000111, doi: 10.1109/OJIM.2023.3239777.

[22] Gurusinghe, D.R. and Rajapakse, A.D., Efficient algorithms for real-time monitoring of transmission line parameters and their performance with practical synchrophasors. IET Generation. Transmission. Distribution., 11: 1134-1143, 2027. https://doi.org/10.1049/iet-gtd.2016.0830

[23] *IEEE/IEC International Standard - Measuring relays and protection equipment - Part 118-1: Synchrophasor for power systems - Measurements*, in IEC/IEEE 60255-118-1:2018 , vol., no., pp.1-78, 19 Dec. 2018, doi: 10.1109/IEEESTD.2018.8577045.

[24] E. Acilan and A. Abur, "Mitigating the Effects of Nonlinear Systematic Errors Within PMU Measurement Infrastructure in Three-Phase Power Systems," in *IEEE Transactions on Power Systems*, vol. 40, no. 3, pp. 2626-2635, May 2025, doi: 10.1109/TPWRS.2024.3496772.

[25] A. G. Phadke and J. S. Thorp, Synchronized Phasor Measurements and Their Applications. Springer, 2011.

[26] P. Denholm, T. Mai, R. Kenyon, B. Kroposki, and M. O'Malley, "Inertia and the Power Grid: A guide without the spin," May 2020. doi: 10.2172/1659820.

979-8-3315-8138-1